C 2 Macromolecular Crowding: Colloidal Suspensions as Models for Biological Systems

P. R. Lang, Y. Liu

ICS-3 Soft Condensed Matter

Institute of Complex Systems

Forschungszentrum Jülich GmbH

Contents

1 Introduction **2**

2 Basics of important theoretical approaches **3**
2.1 Asakura-Oosawa and Vrij theory of depletion interaction 3
2.2 Free volume theory 4
2.3 Scaled particle theory 5

3 Crowding and colloidal phase behavior **6**
3.1 Phase behavior of hard sphere suspensions 6
3.2 Depletion interaction and colloidal phase behavior 9

4 Reaction equilibria and kinetics **10**
4.1 Equilibrium constants 10
4.2 Reaction kinetics 12

5 Conclusions **14**

Lecture Notes of the 49^{th} IFF Spring School "Physics of Life" (Forschungszentrum Jülich, 2018).

1 Introduction

Many biological systems are containing high contents of various macromolecular and colloidal species, they may thus be considered as an aqueous suspension with a high volume fraction of dispersed material. Human blood contains roughly 45 % of cellular material (erythrocytes, leucocytes and thrombocytes) accompanied by about 6-8 % of proteins. The cytoplasm of cells hosts a total volume fraction of the order of 20% of of macromolecules comprising mainly proteins, polysaccharides, DNA and RNA and the nucleus of eucaryotic cells is besides harboring the genome, cramped with bio-polymers of different type and function. Although the concentration of an individual species may be quite low, like thrombocytes and leucocytes, which make less than one percent of the blood volume, the total amount of suspended material can be very large. Such systems are usually called "crowded".

From the perspective of polymer and colloid physics, it is evident that the properties of suspensions and the contained macromolecules will be strongly influenced by their crowded environment. Nevertheless for long time, the standard procedure in the field of biochemistry was to characterize and describe, e. g. proteins on the basis of in vitro experiments carried out in dilute solutions [1]. While the importance of crowding and the resulting excluded volume effects for cell biology was recognized almost four decades ago [2, 3], the significance of crowding for conformation and functioning of biopolymers and entire cells have gained increasing interest only over the last fifteen to twenty years [4, 5] nowadays resulting in several hundreds of scientific papers per year [6].

At mass contents in the range of several hundred mg/mL biological macromolecules do not only interact by site specific interactions but they mutually affect each other by non-specific interactions as van der Waals attraction, hydrophobic and electrostatic interactions as well as excluded volume effects, where the latter are often dominating at physiological conditions. Excluded volume effects usually also referred to as crowding or macromolecular crowding, embrace all properties of macromolecules which are due to the fact that they have less volume available as compared to infinitely dilute suspensions. Under these constraints polymer conformations, diffusion rates, reaction equilibria and kinetics may be drastically different from those occurring in dilute systems. Proteins react to their environment by adjusting their size and shape adopting states spanning from unfolded chains, which resemble ideal polymer coils, to more or less globular assemblies, showing characteristics of nano-particles. In recent years, the impact of crowding onto folding and stability of proteins has been investigated theoretically [7, 8, 9], by computer simulations [10, 11, 12] and experimentally [13, 14, 15, 16].

At sufficiently high concentrations, excluded volume effects can lead to conformational changes and phase separations, which may be leading to the formation of compartments, which coexist in the nuclei of eucaryotic cells despite the absence of separating membranes [17, 18, 19]. Further, inert crowder particles can suppress or promote protein-ligand binding depending on the size and shape ratio between the reaction partners and the product [20, 21].

Beyond the realms of cell biology, concentrated suspensions of biological macromolecules play an important role in various fields. In food industry concentrated mixtures of proteins and polysaccharides are applied in attempts to stabilize water in water emulsions for oil free food formulations [22]. The crowding induced short range order of α-, β- and γ crystalline in the eye lens is of paramount biomedical importance, since it is essential for the lens' transparency [23, 24, 25]. And last but not least the so called depletion effect [26, 27, 28] is applied in protein crystallization for their characterization by x-ray diffraction [29, 30].

Finally the dynamics of macromolecules in the cytoplasm are dictated by crowding to a large

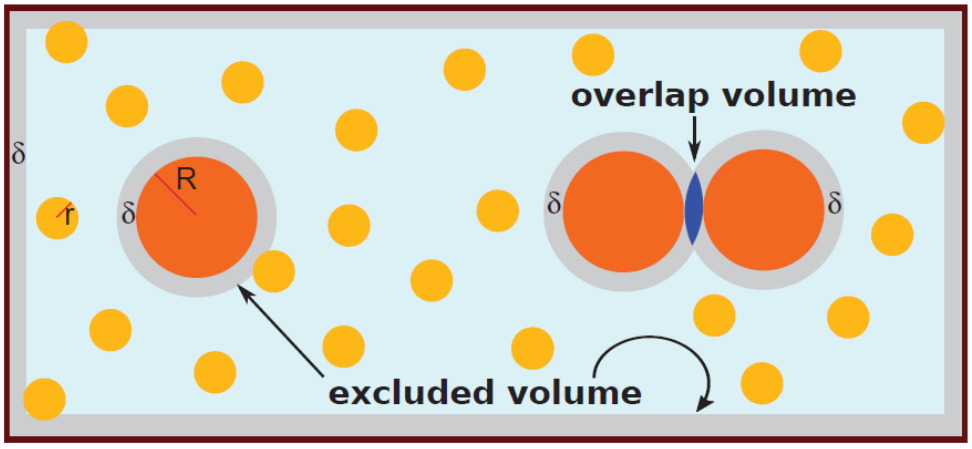

Fig. 1: *Illustration of excluded volume and depletion interaction in a suspension of colloids (big spheres) and depletants (small spheres). The gray areas represent depletion zones, the sum of which together with the volume of all colloids constitutes the excluded volume for the small spheres. Whenever depletion zones overlap (blue area), the excluded volume is reduced by the negative overlap volume and the entropy of the system is increased.*

extend [31, 32, 33]. We will refrain from addressing this subject, as it is discussed in the dedicated chapter D.1 of this book, and even reviewing the plethora of the recent work on static properties in detail is beyond the scope of this contribution. We will rather focus on two major subjects, chosen by personal bias, where we can provide qualitative explanations for some generic features on the the basis of relatively simple approaches from soft matter physics.

2 Basics of important theoretical approaches

2.1 Asakura-Oosawa and Vrij theory of depletion interaction

In any concentrated or crowded suspension, a large part of the available volume is not accessible to particles due to the presence of other particles. Let us consider a colloidal suspension consisting of two types of particles: large spheres and small spheres (depletants), as illustrated in Fig.1. The small spheres can not enter the depletion zones around the large spheres. The sum of the big spheres' volume and the sum of the depletion zones' volumes constitute the volume from which the small spheres are excluded. When two large spheres approach each other, their depletion zones overlap and the total excluded volume is reduced. In other words, the total available volume for small spheres to move freely is increased. The resulting gain of entropy for the system will effectively generate an attractive force between large particles. The scale of the depletion force or potential can be estimated by the Asakura-Oosawa-Vrij theory [26, 27, 28].

For the situation of two kinds of differently sized spheres with radii R_c and r_d the interaction potential between two large spheres can be easily calculated on the bases of geometrical considerations and the assumption that the small spheres thermodynamically behave as an ideal gas

(see for example [34, 35])

$$\frac{\Phi(h)}{k_B T} = \begin{cases} -\rho_d \frac{\pi}{6}(2r_d - h)^2 \left(3R_c + 2r_d + \frac{h}{2}\right) & \text{for} \quad h \leq 2r_d \\ 0 & \text{for} \quad h > 2r_d \end{cases} \quad .. \tag{1}$$

Here h is the surface-to-surface separation between two large spheres, ρ_d is the number density of the small spheres, k_B is Boltzmann's constant and T is the absolute temperature.
If the depletant species is not a sphere but an ideal polymer coil, eq.1 can be used as a good approximation to calculate the pair potential between the large spheres, if the small spheres' diameter is replaced by the thickness of the depletion zone δ, which depends on the ratio of the polymer size over the sphere size, $q = R_g/R_c$. Here R_g is the polymer radius of gyration and

$$\delta = \frac{R_g}{q}\left[\left(1 + \frac{6q}{\sqrt{\pi}} + 3q^2\right)^{1/3} - 1\right] \tag{2}$$

Crowded biological systems are not categorically different from the case of colloidal suspensions. Thus biological macromolecules are subjected to depletion forces which might effect their tendency to form assemblies and their phase behavior.

2.2 Free volume theory

In order to predict phase transitions in crowded systems, a treatment of excluded volume effects on a pair level, as discussed in the preceding section will not be sufficient. The general conditions for two or more phases coexisting are that the chemical potentials of all components in all phases are equal and that the pressure in the coexisting phases is the same. To calculate these properties in systems consisting of colloidal particles and a depleting polymer, the so-called free volume theory [36, 37] was successfully applied. The theory starts from the calculation of the semi-grand potential of a system of N_c colloids and N_d polymers

$$\Omega(V, T, N_c, \mu_d) = F(V, T, N_c, N_d) - \mu_d N_d, \tag{3}$$

where μ_d is the chemical potential of the depletant and $F(V, T, N_c, N_d)$ is the system's Helmholtz free energy at constant composition. We can rewrite this equation as

$$\Omega(V, T, N_c, \mu_d) = F_0(V, T, N_c) - \int N_d(\mu_d) d\mu_d, \tag{4}$$

making use of the thermodynamic relation $(\partial\Omega/\partial\mu_d)_{V,T,N_c} = -N_d$, where $F_0(V, T, N_c)$ is the Helmholtz free energy of the pure colloidal system. Since expressions for the latter are available (see e. g. [34]) we only need to calculate N_d. To this end the system is allowed to osmotically equilibrate with an (infinitely large) reservoir of a depletant solution, via a hypothetical membrane, which is permeable for solvent and depletant molecules, but not for the colloids. By this equilibrium, the chemical potential of the polymer is the same in the reservoir as in all coexistent phases in the system, although the polymer may partition among the phases at different concentrations. Thus

$$\mu_d = \mu_d^0 + k_B T \ln \frac{N_d}{V_{free}} \tag{5}$$

and

$$\mu_d = \mu_d^0 + k_B T \ln \rho_d^R \tag{6}$$

where V_{free} is the total system volume minus the excluded volume and ρ_d^R is the depletant number density in the reservoir. By equating eqs. 5 and 6 we obtain an expression for the number of depletants in the system

$$N_d = \rho_d^R V_{free}. \tag{7}$$

Using the Gibbs-Duhem relation $\rho_d^R d\mu_d = d\Pi^R$ for the osmotic pressure in the reservoir, we can solve the integral in eq. 4 to get

$$\Omega(V, T, N_c, \mu_d) = F_0(V, T, N_c) - \Pi^R V_{free}^0, \tag{8}$$

where we further introduced the main approximation of the theory, by equating the free volume with the free volume in the pure colloid system, V_{free}^0. This implies that the depletants behave as an ideal gas, not causing any excluded volume themselves. Under this assumption, the pressure is also given by the ideal gas analogue $\Pi^R = \rho_d^R k_B T$.
Since for certain size ratios q multiple overlap between depletion zones is possible, their overlapping volumes are not pairwise additive, and the calculation of the free volume is all but trivial. Here we use again the fact that the chemical potential of the depletant is fixed. We can write it as

$$\mu_d = \mu_d^0 + k_B T \ln \frac{N_d}{V} + W \tag{9}$$

where W is the reversible work needed to insert an additional depletant particle into the system. Equating this formulation with eq.5, keeping in mind the approximation $V_{free} = V_{free}^0$, we obtain the fraction of the free volume as

$$\alpha = \frac{V_{free}^0}{V} = \exp\left\{-W/k_B T\right\}. \tag{10}$$

Now the only missing ingredient is the work W, which can be estimated from scaled particle theory as outlined in the next section.

2.3 Scaled particle theory

The scaled particle theory [38] was originally developed to derive expressions for the pressure and the chemical potential of hard sphere fluids by relating them to the reversible work, i. e. the change in free energy, required to introduce an additional sphere to the system, which for our purpose shall have a radius, which is equivalent the thickness of the depletion zone δ. The work is calculated by expanding the radius of the sphere from zero to its final value, i. e. here the radius is $\lambda\delta$ with $0 \leq \lambda \leq 1$. In limit of very small λ it is assumed that there is no overlap of depletion zones, thus the free volume fraction is

$$\alpha = \frac{V - N_c 4\pi (R_c + \lambda\delta)^3/3}{V} \tag{11}$$

which together with eq.10 results

$$\lim_{\lambda \to 0} W(\lambda) = -k_B T \ln\left(1 - \rho_c \frac{4\pi}{3}(R_c + \lambda\delta)^3\right), \tag{12}$$

where ρ_c is the colloid number density in the system. In the other extreme, for very large depletants the work is approximately the volume work needed to create a cavity which is just large enough to accommodate the particle at the given pressure, thus

$$W = \frac{4\pi}{3}(\lambda\delta)^3 \Pi. \tag{13}$$

In the scaled particle theory the work is calculated by expanding the $\lambda \to 0$ limit as a series in λ and adding the value for the large depletant case

$$W(\delta) = W(\lambda \to 0) + \frac{\partial W(\lambda \to 0)}{\partial \lambda}\lambda + \frac{1}{2}\frac{\partial^2 W(\lambda \to 0)}{\partial \lambda^2}\lambda^2 + \frac{4\pi}{3}(\lambda\delta)^3\Pi. \tag{14}$$

After some tedious algebra a complicated but analytical expression for α in dependence of q and the colloid volume fraction ϕ_c is obtained

$$\alpha = (1-\phi_c)\exp\{-U(\phi_c)\} \tag{15}$$

with

$$\begin{aligned} U(\phi_c) &= aQ + bQ^2 + cQ^3 \\ Q &= \phi_c/(1-\phi_c) \\ a &= 3q + 3q^2 + q^3 \\ b &= 9q^2/2 + 3q^3 \\ c &= 3q^3 \end{aligned} \tag{16}$$

This is used to calculate the semi-grand potential, the chemical potential of the colloids and the pressure in the system.

3 Crowding and colloidal phase behavior

In soft matter physics, it is well known that polymer solutions, colloidal suspensions as well as combinations of both may undergo phase transitions of various types, if the solute content is sufficiently increased. In the field of structural biology this effect was long used to achieve protein crystallization for their characterization by x-ray diffraction [29, 30]. The most prominent case of such a phase transition in the field of biology is probably the separation into a protein rich and a protein poor phase in the eye lens cytoplasm, as this is the cause for cataract formation [39, 40, 41, 25]. In cell biology it is speculated that liquid/liquid phase separation is the mechanism by which compartments coexist in the nuclei of eucaryotic cells despite the absence of separating membranes [17, 18, 19]. Therefore, in this chapter we will discuss the fundamentals of phase transitions and coexistence in simple soft matter systems, to set the stage for the much more complex situation in biological environments.

3.1 Phase behavior of hard sphere suspensions

A suspension of spherical particles in a solvent, interacting solely via their excluded volume is termed a hard sphere fluid, if the particle number density, ρ_c, is low. In the very high dilution limit, the system may be regarded as the colloidal analogue to an atomic ideal gas, i. e. the osmotic pressure of the suspension is

$$\Pi = \rho_c k_B T \tag{17}$$

in analogy to the ideal gas law. Like in atomic systems, the particle volume and their interaction potential has to be taken into account to describe the pressure correctly at elevated concentrations. For hard sphere colloids, an accurate description of the osmotic pressure dependence on

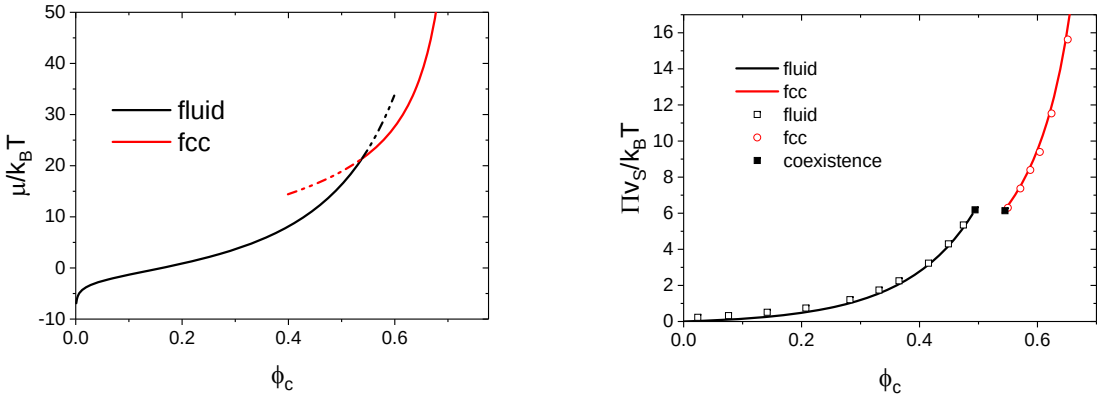

Fig. 2: *Left: Chemical potential in a hard sphere fluid (black) and in a hard sphere fcc-crystalline phase in dependence of volume fraction, as calculated from eqs. 20 and 22. The volume fraction at the intersection is $\phi_c \approx 0.54$. Right: Osmotic pressure of a hard sphere fluid (black) and a hard sphere fcc-crystalline phase (red) in dependence of volume fraction. Full lines are calculated from eqs. 18 and 21 and symbols are from computer simulations [43] where full squares represent the pressure at coexistence [44].*

particle volume fraction is given by the Carnahan-Starling equation of state

$$\widetilde{\Pi} = \frac{\phi_c + \phi_c^2 + \phi_c^3 - \phi_c^4}{(1-\phi_c)^3}, \tag{18}$$

where the dimensionless pressure is $\widetilde{\Pi} = \Pi v_S / k_B T$ with $v_S = 4\pi R_c^3/3$ the volume of a single sphere with Radius R_c. Again, in analogy to atomic systems we expect some kind of phase transition to occur, when the particle volume fraction becomes sufficiently high. At the transition, the pressure and the chemical potential μ of the two coexisting phases have to be equal. To find the transition for the hard sphere system we have thus to have an expression for its chemical potential. This can be obtained from the Gibbs-Duhem relation, which for constant temperature reads $d\Pi = \rho_c d\mu$. With $\rho_c = \phi_c / v_S$ the chemical potential can formally be written as

$$\int d\mu = \mu = \mu^0 + v_S \int_0^{\phi_c} \frac{1}{\phi_c'} \frac{d\Pi}{d\phi_c'} d\phi_c' \tag{19}$$

where the ideal gas reference term $\mu^0 = k_B T ln\,(\Lambda^3/v_S)$ with the particles De Broglie wavelength $\Lambda = h\sqrt{2\pi m_S k_B T}$, h Planck's constant and m_S the single particle mass [42]. Calculating $d\Pi/d\phi_c$ from eq. 18 and solving the integral on the right hand side, the dimensionless chemical potential $\widetilde{\mu} = \mu / k_B T$ is obtained as:

$$\widetilde{\mu} = ln\frac{\Lambda^3}{v_S} + ln\phi_c + \frac{3-\phi_c}{(1-\phi_c)^3} - 3. \tag{20}$$

Theoretical and simulation studies in the mid of the twentieth century revealed that hard spheres fluid will transform into a face centered cubic ordered system at sufficiently large volume fractions. Analytical approximations for the pressure

$$\widetilde{\Pi}_{fcc} = \frac{3\phi_c}{1 - \phi_c/\phi_{cp}} \tag{21}$$

Fig. 3: *PMMA particles suspended in an refractive index matching solvent mixture at effective volume fractions indicated by the numbers at the bottom. The samples are illuminated obliquely from behind with white light. Homogeneous colors indicate a random distribution of particles while opacity is due to Bragg diffraction, indicating crystal structures with lattice constants in the wave length range of visible light. Image reproduced from reference [45] with permission.*

and the chemical potential

$$\widetilde{\mu}_{fcc} = ln\frac{\Lambda^3}{v_S} + \frac{27}{8\phi_{cp}^3} + 3ln\left(\frac{\phi_c}{1-\phi_c/\phi_{cp}}\right) + \frac{3}{1-\phi_c/\phi_{cp}} \tag{22}$$

, of this ordered system can be found in, e. g. reference [34] together with a comprehensive derivation of the entire subject. Here $\phi_{cp} \approx 0.74$ is the volume fraction at crystalline close packing of spheres .

As shown in the left panel of Fig. 2, the two curves representing eqs. 20 and 22 intersect at $\phi_c \approx 0.54$. This value is indicating the highest volume fraction up to which the fluid state of the hard sphere system can exist, since the condition for coexisting phases is $\widetilde{\mu} = \widetilde{\mu}_{fcc}$. At this volume fraction, the pressure of the ordered system has its minimal, i. e. the coexistence value $\Pi_{coex} \approx 6.0$. According to eq. 18 the fluid system reaches this pressure at a volume fraction of $\phi_c \approx 0.49$ as shown in the right panel of Fig. 2, where we compare the calculated data according to eqs. 20 and 22 to results of computer simulations [44, 43].

An experimental verification of the fluid to crystal transition in a quasi hard sphere colloidal system is displayed in Fig. 3, which shows an image of samples containing increasing volume fractions of colloidal spheres in an index matching solvent mixture [45]. The samples are illuminated obliquely from behind with white light, which results in an opaque appearance due to Bragg diffraction, if there is long range order. Samples or parts of the samples showing homogeneous color have a fluid like structure. Thus, below an effective volume fraction of ~ 0.5 the sample is completely isotropic, while in the range $0.51 < \phi < 0.53$ a fluid coexists with a crystalline structure. Up to $\phi \leq 0.58$ the samples are fully crystalline while at even higher volume fractions a new isotropic state occurs, which is a colloidal glass.

It is important to note that even the apparently simple system of hard colloidal spheres undergoes phase separation at sufficiently high concentrations. However, there is no phase coexistence of a gas-like and a liquid-like phase, thus the hard sphere fluid is always super-critical.

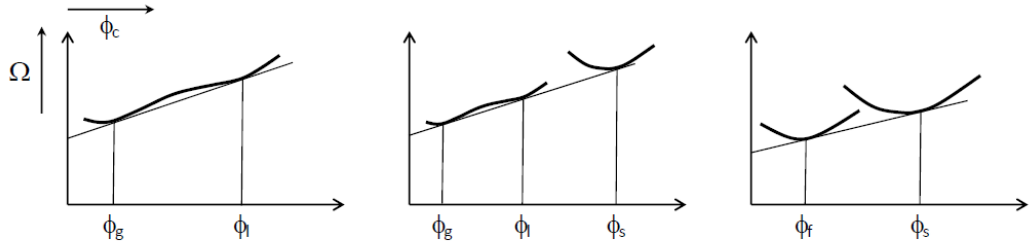

Fig. 4: *Sketch of the semi-grand potential in dependence of the colloid volume fraction in a colloid-polymer mixture. The common tangents connect points of equal slopes, identifying the the colloid volume fraction of coexisting phases. Left: gas-like/liquid-like coexistence; middle: three phase coexistence of a gas-like, a liquid-like and a solid-like state; right: coexistence of a supercritical fluid state with a crystalline state.*

To induce a gas/liquid-like phase coexistence, attractive interactions between the particles are required, which we will discuss in the next section.

3.2 Depletion interaction and colloidal phase behavior

In crowded systems, particle-particle interactions will become more and more important the higher the macromolecular contents. In experimental model systems, electrostatic interactions can be reduced by adding large amounts of electrolytes and van der Waals interactions can be minimized by adjusting the solvent's refractive index to that of the suspended particles. Differently, depletion interactions will inevitably occur, due to excluded volume interactions. To predict the phase diagram of such systems, the semi-grand potentials, Ω, of the various possible states of the system have to be calculated numerically, using free volume theory. Since the chemical potential of a component is the derivative of the semi-grand potential with respect to its concentration, the slope of a Ω vs. ϕ curve is a chemical potential. This is illustrated in Fig. 4 where we sketch the semi-grand potential in dependence of the colloid volume fraction ϕ_c in a colloid polymer mixture for three different situations. To identify the colloid content of coexisting phases, conditions have to be identified by the common tangent (the thin, non vertical lines in the graphs) construction, connecting the points of the curves with equal slope, indicating identical chemical potentials of the colloid $\mu_c^I = \mu_c^{II}$ in the coexisting phases.
According to standard thermodynamics $\Omega = -\Pi V + \mu N$. Thus, the system pressure at coexistence is related to the intercept of the common tangent. In the left panel of Fig. 5 we show a phase diagram in the ϕ_d^R–ϕ_c plane of a polymer-colloid mixture at $q = 0.6$, where ϕ_d^R is the depletant polymer volume fraction in a reservoir. The plot represents a comparison of results calculated using free volume theory [36] with data from computer simulations [46]. At volume fractions of polymer and colloid, which are both below ~ 0.5 the mixture consists of a single liquid-like phase. If the polymer volume fraction is $0.5 \lesssim \phi_d^R \lesssim 1.3$ the system separates into a gas-like phase, coexisting with a liquid-like phase and at polymer volume fractions $\phi_d^R \gtrsim 1.3$ a supercritical fluid is coexisting with the crystalline phase. For colloid volume fractions $\phi_c \gtrsim 0.55$ the system is in the crystalline state, independent of the polymer content. A triple point , at which the three phases coexist is located at $\phi_c \approx 0.5$ and $\phi_d^R \approx 1.3$.
An experimental example for this behavior is displayed in the right panel of Fig. 5. The samples shown, contain polystyrene latex particles with $R_c = 67$nm at a volume fraction $\phi_c = 0.16$ and

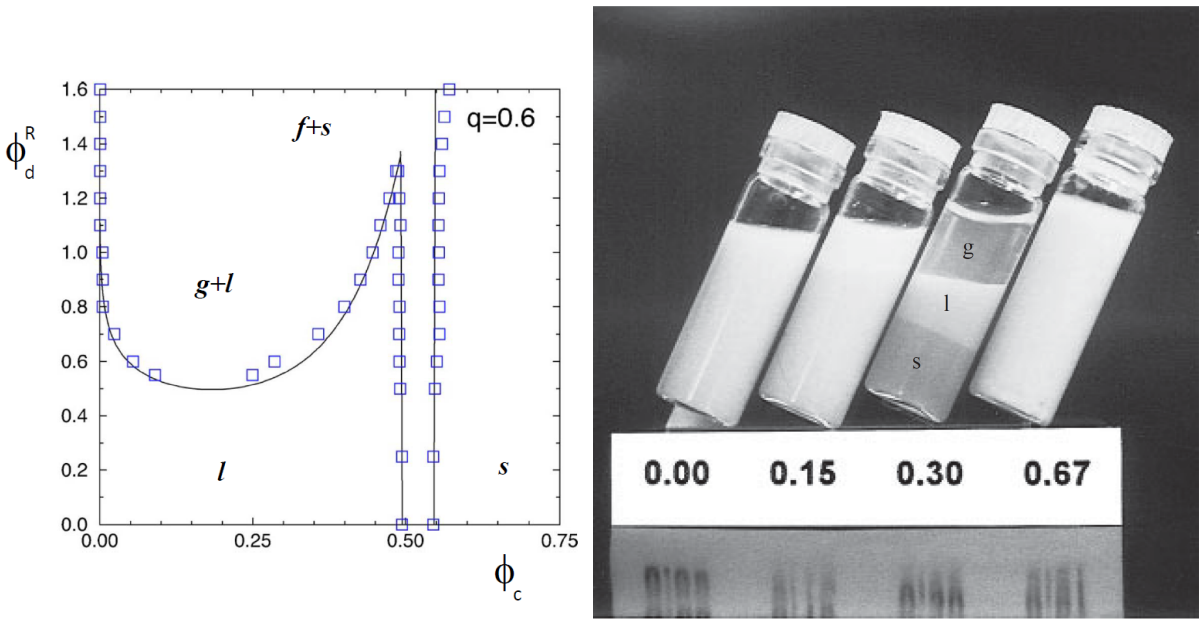

Fig. 5: *Left: Phase diagram of a colloid polymer mixture in the ϕ_p^R-ϕ_c-plane at $q = 0.6$. Full lines were calculated using free volume theory [36] and symbols are data from computer simulations (reproduced with permission from reference [46]). Right: Image of 67 nm polystyrene latex aqueous suspensions with different amounts of hydroxyethylcellulose (HEC), indicated as weight per volume percentage by the numbers at the bottom. The sample with 0.3 %w/v shows the coexistence of a solid, a liquid-like and a gas-like phase (reproduced with permission from reference [47]).*

hexaethylcellulose (HEC) as the polymeric depletant at concentrations which are indicated in units of % (w/v). The sample containing 0.3% HEC, obviously has the triple point composition, as three phases are clearly visible. The top phase boundary remains horizontal, if the sample is tilted, showing that the two adjacent phases are fluid. Differently, the lower phase boundary follows the inclination of the vial, showing that the bottom phase has solid-like properties.

4 Reaction equilibria and kinetics

4.1 Equilibrium constants

Most proteins and other biopolymers in living cells assemble into compound structures or pass through transient complexes, to execute their designed function. It is obvious that attractive interactions among the constituents will favor the development of these complexes. However, also excluded volume effects my have a pronounced effect on their formation. It is difficult to measure these unspecific contributions directly, but their effect can be observed indirectly by determining equilibrium constants [48, 49, 50, 51, 52] and reaction rates [53, 54, 55, 56].
Many of these effects can be predicted quantitatively, using thermodynamic approaches. Here we will discuss the change of the equilibrium constant for the association of the two species A and B into a complex AB. In Fig. 6 we show a thermodynamic cycle, which basically consist of four steps (i) the association/dissociation reaction in dilute solution, (ii) the transfer of the product from the dilute system into a crowded environment, (iii) the association/dissociation

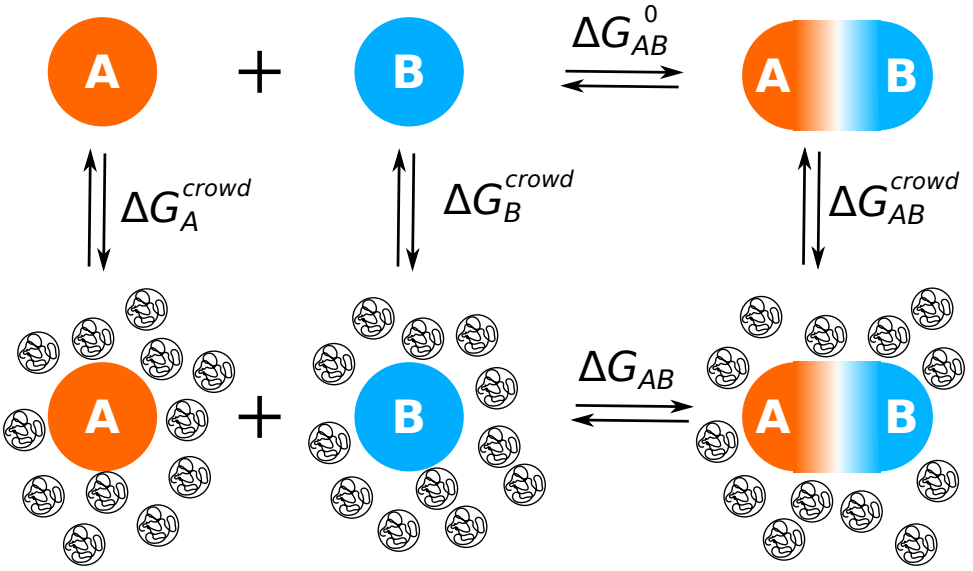

Fig. 6: *Thermodynamic cycle demonstrating the difference between the standard reaction free energy, ΔG^0_{AB}, in dilute solution and the free energy change, ΔG_{AB}, of the same reaction in a crowded environment. The difference is determined by the changes of free energy ΔG_X^{crowd}, connected to transferring the species $X \in A, B, AB$ from a dilute solution to a crowded suspension.*

reaction in the crowded environment and (iv) the transfer of the reactants from the crowded environment back into the dilute solutions. Since the change of Gibbs free energy along this circular path has to be zero, we realize that the difference between the reaction free energy in the crowded system and the standard reaction free energy is

$$\Delta\Delta G_{AB} \equiv \Delta G_{AB} - \Delta G^0_{AB} = \Delta G^{crowd}_{AB} - \Delta G^{crowd}_{A} - \Delta G^{crowd}_{B} \tag{23}$$

where ΔG_X^{crowd} is the molar work it takes to transfer the species X, which comprises A, B and AB, from a dilute solution to the crowded environment. Approximating the reactants and the formed complex as convex spheroid bodies, we can calculate this work applying results from scaled particle theory [38, 57, 58]. The work required to accommodate a spherocylinder with a tip-to-tip length L and a cross section radius R_{cs}, which is equal to the radius of the hemispherical end-caps, into a suspension of hard spherical particles with radius R_1 at volume fraction ϕ is approximately given by

$$\frac{\Delta G_X^{crowd}}{RT} = -ln(1-\phi) + A_1 Q + A_2 Q^2 + A_3 Q^3 \tag{24}$$

where R is the gas constant, $Q = \phi/(1-\phi)$ is the ratio of the volume occupied by the particles over the unoccupied volume and

$$\begin{aligned} A_1 &= R_{cs}^3 + 3R_{cs}^2 + 3R_{cs} + \frac{3}{2}(l+1)(R_{cs}^2 + 2R_{cs} + 1) \\ A_2 &= \frac{3}{2}(2R_{cs}^3 + 3R_{cs}^2) + \frac{9}{2}(l+1)(R_{cs}^2 + R_{cs}) \\ A_3 &= 3R_{cs}^3 + \frac{9}{2}(l+1)R_{cs}^2. \end{aligned} \tag{25}$$

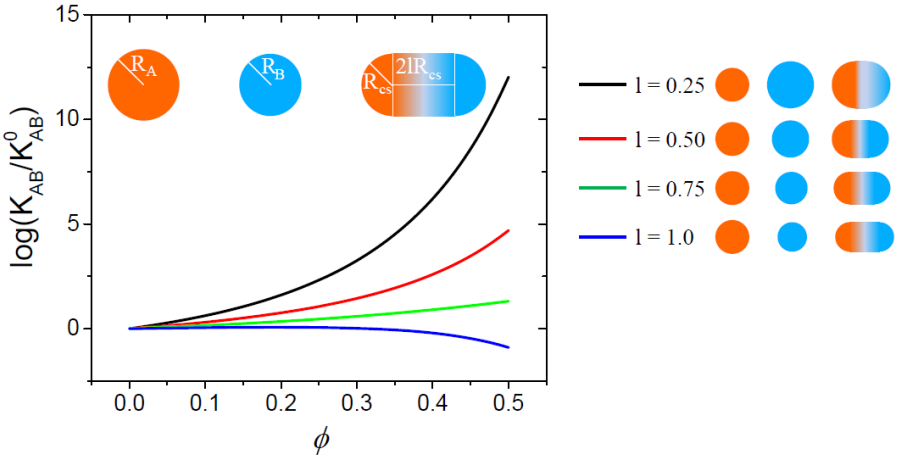

Fig. 7: *Variation of the equilibrium constant for the formation of a spherocylindrical complex from two spherical reactants in dependence of volume fraction of spherical crowders with same radius as sphere A. Different colors of the full lines refer to various aspect ratios of the product as indicated in the panel at the right.*

Here l is the length of the right cylinder, i. e. the spherocylinder without the end-caps, expressed in units of the cross section radius $l = L/2R_{cs} - 1$, thus $l = 0$ represents the case of a sphere with radius R_{cs}.
Let us now consider an association reaction between two particles, one with radius $R_A = R_1$ the other with radius $R_B = rR_1$ into a spherocylindrical object with $R_{cs} = R_B$ and various length, demanding that the volume of the spherocylinder shall be equal to the sum of the volumes of the two reactant spheres which requires that $l = 2/3r^3$. The equilibrium constants of the reaction in dilute solution, K^0_{AB}, and in the crowded environment, K_{AB}, and their ratio are given by standard chemical thermodynamics as

$$\begin{aligned} K^0_{AB} &= \exp\left\{-\Delta G^0_{AB}/RT\right\} \\ K_{AB} &= \exp\left\{-\Delta G_{AB}/RT\right\} \\ \frac{K_{AB}}{K^0_{AB}} &= \exp\left\{-\Delta\Delta G_{AB}/RT\right\} \end{aligned} \tag{26}$$

Result for the ratio of equilibrium constants are shown in Fig. 7. Obviously crowding can increase the tendency of species A and B to associate, when the resulting complex is rather compact, i. e. $l \to 0$. On the other hand crowding may hamper association, if the dimer becomes increasingly elongated. In this case the resulting complex excludes more volume to the crowder than the two reactant spheres. For systems in which a larger number, N, of proteins associate, similar effects are predicted, which increase drastically with N [59].

4.2 Reaction kinetics

The kinetics of association reactions are dominated mainly by two effects, the diffusion of reactants which controls the the probability of two reactants meeting and the energy barrier related to the formation of intermediate reaction states. According to the two extreme cases, the reaction rate in diffusion limited cases and in transition-state controlled situations is here called

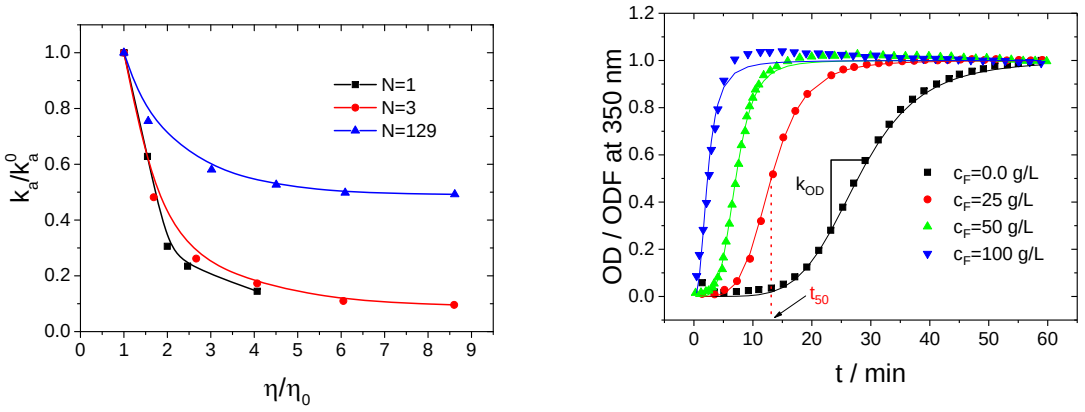

Fig. 8: *Left: Effect of PEG chain length on the rate constant of the BLIB dimerization. Rate constants, normalized by the rate constant in pure buffer, are plotted versus the solvent viscosity, normalized by the viscosity of the pure buffer, for solutions containing PEG with different chain length, N, as indicated in the legend. Points represent experimental data reproduced from reference [53] and lines are guides to the eye. Right: Sample turbidity as a function of time following the polymerization reaction of HIV-1 capsid protein in suspensions with various contents c_F of the synthetic crowding agent Ficoll 70. Symbols represent data reproduced from reference [54] and the lines are best fits with the Hill-function [62].*

k_d and k_t, respectively. In general the reaction rate of the association can be approximated by a a combination of the two limiting cases [60] as

$$k_a = \frac{k_d k_t}{k_D + k_t} \tag{27}$$

In the two limiting cases, the rate constants depend in different ways on crowding. As k_d is proportional to the reactants mobility in its surrounding, increasing volume fractions of crowders are expected to cause a monotonic decrease of k_d. At the same time depletion causes an effective attraction between the reactants, favoring dimerization, which may partially counterbalance but generally not overcompensate the effect of decreasing k_d. It is argued that k_t should increase with crowding, because crowding will favor the formation of compact transition states thereby lowering the energy barrier for their formation. Thus the association rate constant should increase by a similar amount as the equilibrium constant of the association reaction. As a rule of thumb, fast associations are usually diffusion limited, while slow associations are dictated by the energy barrier of the transition state [61]. Therefore, crowding is generally expected to slow down fast and to accelerate slow reactions.

Examples for both limits are shown in Fig. 8. In the left panel the effect of buffer viscosity and crowding on the rate constant for the dimerization of β-lactamase inhibitor protein (BLIB) is demonstrated. Rate constants, normalized by the rate constant in pure buffer are plotted versus the normalized viscosity of the suspending solution, which contains poly-ethylene-glycol (PEG) with different degrees of polymerization, N. In ethylene-glycol ($N = 1$) and in PEG-200 ($N \approx 3$) solution, the reaction rates are significantly decreased due to increasing viscosity of the solvent, which results in a corresponding reduction of the BLIP diffusion constant. However, in PEG-8000 solution ($N \approx 130$) the polymer coils are large enough to cause significant attractive depletion interaction between the proteins, favoring association and thereby counterbalancing the effect of decreasing k_d to a large extent.

In the right panel the optical density of suspensions of Human Immunodeficiency Virus Type 1 Capsid Protein (HIV-1 CA) is plotted as a function of time after triggering their assembly reaction by the addition of the crowding agent Ficoll70, which is a highly branched copolymer of saccharose and epichlorohydrin. As the total content of HIV-1 CA in the sample is constant over time, the turbidity is a rough measure for the average size of the assemblies in the solution. Either the inverse of the time t_{50}, at which the optical density reaches half of its final value $OD = 0.5ODF$, or the rate of change of the optical density k_{OD} in the region where OD depends more or less linear on time, is a measure for the rate constant of the assembly reaction. It is thus obvious that the reaction is significantly sped up by the presence of the crowder, which is just occupying volume and increasing the system viscosity, being inert in any other respect.

5 Conclusions

In may biological systems, like blood, cytoplasm or the nuclei of eucaryotic cells there is a large volume fraction of macromolecular solutes, inevitably causing excluded volume interactions. These can drastically alter the structure and the functioning of biological macromolecules, as compared to their properties in dilute suspensions.

Here we have discussed that excluded volume effects will lead to colloidal phase transition and the coexistence of various phases at volume fractions which are typical for many biological system. It is thus speculated that phase separation, due to macromolecular crowding is the basis for micro-compartmentation in cytoplasm and nucleoplasm.

Further protein function is strongly influenced by macromolecular crowding, by e. g. fostering reactions, leading to the reduction of total excluded volume. However, the magnitude of the effect is expected to dependent drastically on the relative size and shape of the involved species. Finally we demonstrated that reaction rates are influenced by crowding effects. Generally we may expect that fast, diffusion limited reactions are slowed down by crowding while slow, transition state- controlled reactions are sped up.

References

[1] G. B. Ralston, J. Chem. Edu. **67**(10), 857 (1990).

[2] A. P. Minton, Biophysical Journal **31**(1), 77 (1980).

[3] A. P. Minton, Biochemistry **20**, 4821 (1981).

[4] R. J. Ellis, Trends in biochemical sciences **26**(10), 597 (2001).

[5] R. J. Ellis, Current opinion in structural biology **11**(1), 114 (2001).

[6] G. Foffi, Phys. Biol. **10**, 040301 (2013).

[7] A. P. Minton, Biophys. J. **78**, 101 (2000).

[8] A. P. Minton, Curr.Opin. Struct. Biol. **10**, 34 (2000).

[9] A. P. Minton, Biophys. J. **88**, 971 (2005).

[10] M. S. Cheung, D. Klimov, and D. Thirumalai, Proc. Natl. Acad. Sci. **102**, 4753 (2005).

[11] M. S. Cheung, Current Opin. Struct. Biol. **23**, 1 (2013).

[12] T. Hoppe and J.-M. Yuan, J. Phys. Chem. B **115**, 2006 (2011).

[13] A. P. Schlesinger, Y. Wang, X. Tadeo, O. Millet, and G. J. Pielak, Journal of the American Chemical Society **133**(21), 8082 (2011).

[14] E. Chen, A. Christiansen, Q. Wang, M. S. Cheung, D. S. Kliger, and P. Wittung-Stafshede, Biochemistry **51**(49), 9836 (2012).

[15] Y. Wang, M. Sarkar, A. E. Smith, A. S. Krois, and G. J. Pielak, Journal of the American Chemical Society **134**(40), 16614 (2012).

[16] L. A. Benton, A. E. Smith, G. B. Young, and G. J. Pielak, Biochemistry **51**(49), 97739775 (2012).

[17] H. Walter and D. E. Brooks, FEBS letters **361**(2-3), 135 (1995).

[18] R. Hancock, Biol. Cell **96**, 595 (2004).

[19] W. M. Aumiller Jr, B. W. Davis, and C. D. Keating, Int. Rev. Cell Mol. Biol **307**, 109 (2013).

[20] H.-X. Zhou, Journal of Molecular Recognition **17**(5), 368 (2004).

[21] H.-X. Zhou, G. Rivas, and A. P. Minton, Annu. Rev. Biophys. **37**, 375 (2008).

[22] M. Vis, J. Opdam, I. S. J. van t Oor, G. Soligno, R. van Roij, R. H. Tromp, and B. H. Ern, ACS Macro Letters **4**(9), 965 (2015).

[23] G. B. Benedek, Appl. Opt. **10**, 459 (1971).

[24] M. Delaye and A. Tardieu, Nature **302**, 415 (1986).

[25] G. Foffi, G. Savin, S. Bucciarelli, N. Dorsaz, G. M. Thurston, A. Stradner, and P. Schurtenberger, Proceedings of the National Academy of Sciences **111**(47), 16748 (2014).

[26] S. Asakura and F. Oosawa, J. Chem. Phys. **22**, 1255 (1954).

[27] S. Asakura and F. Oosawa, J. Polym. Sci **33**(126), 183 (1958).

[28] A. Vrij, Pure Appl. Chem. **48**, 471 (1976).

[29] S. D. Durbin and G. Feher, Annu. Rev. of Phys. Chem. **47**, 171 (1996).

[30] J. Blouwolff and F. Seth, Journal of Crystal Growth **303**, 546 (2007).

[31] E. Zhou, X. Trepat, C. Park, G. Lenormand, M. Oliver, S. Mijailovich, C. Hardin, D. Weitz, J. Butler, and J. Fredberg, Proceedings of the National Academy of Sciences **106**(26), 10632 (2009).

[32] M. A. Mourão, J. B. Hakim, and S. Schnell, Biophysical journal **107**(12), 2761 (2014).

[33] B. R. Parry, I. V. Surovtsev, M. T. Cabeen, C. S. OHern, E. R. Dufresne, and C. Jacobs-Wagner, Cell **156**(1), 183 (2014).

[34] H. N. W. Lekkerkerker and R. Tuinier, *Colloids and the Depletion Interaction*, vol. 833 of *Lecture Notes in Physics* (Springer, Dordrecht, Heidelberg, London, New York, 2011).

[35] P. R. Lang, D. Vlassopoulos, and W. Richtering, *Polymer Science: A Comprehensive Reference* (Elsevier, Amsterdam, The Netherlands, 2012), chap. Polymer/Colloid Interactions and Soft Polymer Colloids.

[36] H. N. W. Lekkerkerker, W. C.-K. Poon, P. N. Pusey, A. Stroobants, and P. B. Warren, EPL (Europhysics Letters) **20**(6), 559 (1992).

[37] G. J. Fleer and R. Tuinier, Advances in Colloid and Interface Science **143**(1-2), 1 (2008).

[38] H. Reiss, H. L. Frisch, and J. L. Lebowitz, The Journal of Chemical Physics **31**, 369 (1959).

[39] M. L. Broide, C. R. Berland, J. Pande, O. O. Ogun, and G. B. Benedek, Proceedings of the National Academy of Sciences **88**(13), 5660 (1991).

[40] C. Liu, N. Asherie, A. Lomakin, J. Pande, O. Ogun, and G. B. Benedek, Proceedings of the National Academy of Sciences **93**(1), 377 (1996).

[41] N. Dorsaz, G. M. Thurston, A. Stradner, P. Schurtenberger, and G. Foffi, Soft Matter **7**, 1763 (2011).

[42] D. A. Mc Quarrie, *Statistical Mechanics* (University Science Books, Sausalito, 2000).

[43] A. Fortini, M. Dijkstra, and R. Tuinier, J. Phys.: Condens. Matter **17**(50), 77837803 (2005).

[44] W. G. Hoover and F. H. Ree, J. Chem. Phys. **49**, 3609 (1968).

[45] P. N. Pusey and W. van Megen, Nature **320**, 340 (1986).

[46] M. Dijkstra, R. van Roij, R. Roth, and A. Fortini, Phys. Rev. E **73**, 041404 (2006).

[47] M. A. Faers and P. F. Luckham, Langmuir **13**(11), 2922 (1997).

[48] H. J. Bosma, G. Voordouw, A. De Kok, and C. Veeger, FEBS Letters **120**, 179 (1980).

[49] J. Wilf and A. P. Minton, Biochimica et Biophysica Acta (BBA) - Protein Structure **670**(3), 316 (1981).

[50] S. B. Zimmerman and S. O. Trach, Nucleic Acids Research **16**(14A), 6309 (188).

[51] T. Díaz-López, C. Dávila-Fajardo, F. Blaesing, M. P. Lillo, and R. Giraldo, Journal of Molecular Biology **364**(5), 909 (2006).

[52] X. Aguilar, C. F. Weise, T. Sparrman, M. Wolf-Watz, and P. Wittung-Stafshede, Biochemistry **50**(14), 3034 (2011).

[53] N. Kozer and G. Schreiber, Journal of Molecular Biology **336**(3), 763 (2004).

[54] M. del Álamo, G. Rivas, and M. G. Mateu, J. Virol. **79**(22), 14271 (2005).

[55] Y. Phillip, E. Sherman, G. Haran, and G. Schreiber, Biophysical Journal **97**(3), 875 (2009).

[56] Y. Phillip and G. Schreiber, FEBS Letters **587**(8), 1046 (2013).

[57] M. A. Cotter, J. Chem. Phys. **66**, 1098 (1977).

[58] G. Rivas, J. A. Fernández, and A. P. Minton, Proceedings of the National Academy of Sciences **98**(6), 3150 (2001).

[59] A. P. Minton, Biopolymers **20**(10), 2093 (1981).

[60] H. Zhou and A. Szabo, Biophysical Journal **71**(5), 2440 (1996).

[61] R. Alsallaq and H.-X. Zhou, Biophysical Journal **92**(5), 1486 (2007).

[62] A. V. Hill, J. Physiol. **40**, 4 (1910).